coatings

MDPI

*Article*

# Comparative Effects of Tung Oil/Chitosan–Gum Arabic Microcapsules Prepared Under Two Feed Efficiencies on Surface Coating Performance of Bamboo

**Xiang Liu [1,2], Jingyi Hang [1,2], Hongxia Yang [1,2], Xiaoxing Yan [1,2,*] and Jun Li [1,2]**

[1] Co-Innovation Center of Efficient Processing and Utilization of Forest Resources, Nanjing Forestry University, Nanjing 210037, China; liuxiang@njfu.edu.cn (X.L.); hangjingyi@njfu.edu.cn (J.H.); yanghongxia@njfu.edu.cn (H.Y.); lijun0099@njfu.edu.cn (J.L.)
[2] College of Furnishings and Industrial Design, Nanjing Forestry University, Nanjing 210037, China
* Correspondence: yanxiaoxing@njfu.edu.cn

## Abstract

Bamboo surfaces are susceptible to scratches and contamination during service, which limits their durability and aesthetic performance. To address this issue, this study aims to develop a natural self-healing coating based on tung oil microcapsules. Tung oil microcapsules encapsulated within chitosan and gum arabic (TO/CS–GA MCs) were prepared by spray drying at two feed rates (100 and 200 mL $h^{-1}$) and incorporated into tung oil coatings applied on bamboo substrates. The effects of microcapsule content (1.0–11.0 wt%) and feed rate on the optical performance, mechanical performance, and self-healing performance of the coatings were systematically investigated. The results showed that increasing the microcapsule content gradually increased the color difference ($\Delta E$) and surface roughness of the coatings, while the gloss decreased. The hardness, impact resistance, adhesion grade, and self-healing efficiency of the coatings exhibited a similar trend, initially increasing and then decreasing with increasing microcapsule content. This behavior indicates that an appropriate amount of microcapsules can enhance the coating performance, whereas excessive addition leads to particle agglomeration and structural defects. Under the better condition of 5.0 wt% microcapsule content and a spray-drying feed rate of 100 mL $h^{-1}$, the coating exhibited the best overall performance, including higher gloss retention, a hardness of 2H, an impact resistance of 3 kg·cm, relatively low surface roughness, and a self-healing efficiency of 28.16 ± 0.63%. These results suggest that the spray-drying feed rate plays an important role in regulating the particle size distribution and encapsulation efficiency of the microcapsules, which in turn affects their dispersion and rupture–release behavior within the coating matrix. Therefore, controlling the spray-drying parameters is crucial for optimizing the performance of microcapsule-based self-healing coatings. Overall, this study provides a sustainable strategy for developing natural polymer-based self-healing coatings and offers useful insights into the design of functional microcapsules for bamboo surface protection.

**Keywords:** bamboo coatings; microcapsules; self-healing; spray drying; tung oil

Check for updates

Academic Editor: Flavio Deflorian

Received: 23 March 2026
Revised: 11 April 2026
Accepted: 15 April 2026
Published: 16 April 2026

**Copyright:** © 2026 by the authors. Licensee MDPI, Basel, Switzerland. This article is an open access article distributed under the terms and conditions of the Creative Commons Attribution (CC BY) license.

## 1. Introduction

Bamboo is a rapidly renewable biomass resource with a short growth cycle and a relatively low carbon footprint. Owing to its favorable mechanical performance, high strength-to-weight ratio, and environmental sustainability, bamboo has attracted increasing

attention in applications such as construction, furniture manufacturing, and interior decoration [1–3]. However, during practical service, bamboo surfaces are prone to scratches, abrasion, and contamination caused by daily friction or accidental impacts. These defects not only deteriorate the visual appearance of bamboo products but also accelerate surface degradation and shorten their service life. With the increasing demand for environmentally friendly and durable household materials, the development of protective coatings with enhanced durability and self-healing capability has become an effective strategy to improve the service performance of bamboo materials.

Microencapsulation technology has attracted extensive interest due to its ability to encapsulate functional substances and regulate their release behavior [4]. By forming a protective shell around an active core material, microcapsules can effectively isolate sensitive components, stabilize functional substances, and improve the overall performance of composite systems. As a result, this technology has been widely explored in diverse fields, including energy-saving materials, pharmaceuticals, and military camouflage systems [5–7]. In general, microcapsules are prepared by coating a core material with a polymer shell to achieve controlled release functionality, and the fabrication approaches can be broadly classified into three categories. The first category includes chemical methods, such as interfacial polymerization, which have been used to produce phase-change microcapsules with a latent heat of 100.21 $\pm$ 2.7 J/g as well as self-healing microcapsules [8,9]. The second category involves physical methods based on mechanical processes, including spray drying and solvent evaporation techniques [10,11]. The third category is physicochemical methods, in which the solubility of polymers is reduced through the addition of solvents, salts, electrolytes, or by adjusting parameters such as temperature and pH, allowing the polymer to deposit on the core material surface and form a shell layer. Typical examples include phase separation methods, ion exchange and Stöber processes, and complex coacervation techniques [12–15]. The selection of shell materials is critical for microcapsule formation; suitable shell materials should exhibit good film-forming ability, sufficient mechanical strength, ease of processing, low cost, and minimal toxicity. Generally, shell materials can be categorized into natural polymers, semi-synthetic polymers, and synthetic polymers. The choice of core material depends on the functional requirements of the microcapsules. For self-healing systems, the core material typically needs to possess adequate fluidity so that it can flow into damaged regions after release. Common healing agents include drying vegetable oils and isocyanates [16,17]. In addition, emulsifiers play a key role in stabilizing the emulsion system during microcapsule fabrication. Their type and dosage significantly influence the emulsification efficiency and ultimately determine the particle size and stability of the resulting microcapsules. Therefore, appropriate emulsifiers must be selected according to the specific core material in order to improve the microcapsule yield and performance. For instance, previous studies have shown that using sodium dodecyl benzene sulfonate (SDBS) as an emulsifier can produce microcapsules with uniform particle size and improved thermal stability [18]. Since their first application in carbonless copy paper in 1954, microcapsule technologies have undergone rapid development, and the concept of self-healing microcapsules was later pioneered by the White research group and subsequently extended to applications such as concrete and marine coatings [19].

Tung oil, a natural drying oil extracted from the seeds of Vernicia fordii, exhibits an excellent oxidative self-polymerization ability [20]. Through the conjugated double bonds in its molecular structure, tung oil can undergo free-radical oxidative crosslinking reactions in air, forming a dense and stable coating with good fluidity and film-forming properties. Compared with synthetic healing agents, tung oil is widely available, environmentally friendly, non-toxic, and biodegradable, which makes it consistent with the development trend of sustainable coating materials. Chitosan, a natural polysaccharide derived from

chitin, contains abundant amino and hydroxyl functional groups, which endow it with excellent film-forming ability, biocompatibility, and mechanical strength [21]. Gum arabic is another natural polysaccharide that exhibits excellent emulsifying stability and water solubility [22]. Due to the electrostatic interactions between chitosan and gum arabic, these two biopolymers can form a stable composite shell structure, which can improve the encapsulation efficiency of microcapsules and enhance the mechanical stability of the shell wall [23]. At present, microcapsules are commonly prepared using emulsion-based methods. However, these methods still suffer from several limitations, including low preparation efficiency, complex separation and drying processes, and the tendency of microcapsules to agglomerate, which restricts their large-scale industrial application [24]. In contrast, spray drying has attracted increasing attention as an efficient microencapsulation technique due to its high preparation efficiency, continuous production capability, easy scalability, and good dispersibility of the resulting microcapsules. In particular, spray drying is highly suitable for microcapsules with natural polymer shell materials [25,26]. Previous studies have investigated the application of microcapsule-based self-healing coatings for wood substrates [27–29]. For instance, Dong et al. prepared tung oil microcapsules using chitosan and sodium tripolyphosphate and demonstrated that the incorporation of such microcapsules could improve the durability of wood coatings [27]. In addition, Chang et al. summarized the recent progress of self-healing microcapsules used in wood coatings and highlighted the importance of microcapsule structure and dispersion in improving coating performance [29]. Nevertheless, most previous studies mainly focused on the selection of shell materials and core materials, whereas the influence of spray-drying parameters, particularly feed rate, on the microstructure of microcapsules and the resulting coating performance has rarely been systematically investigated [4,27]. Therefore, in this study, tung oil microcapsules encapsulated within chitosan and gum arabic (TO/CS–GA MCs) were prepared using a spray-drying technique. To highlight the influence of feed rate on atomization behavior and drying kinetics, two representative feed rates (100 and 200 mL $h^{-1}$) were selected for comparison in order to generate distinct differences in microcapsule structure and coating performance. The prepared microcapsules were incorporated into tung-oil-based coatings applied on bamboo substrates. Subsequently, the optical performance, mechanical performance, and self-healing performance of the coatings were systematically evaluated. This study aims to clarify the relationship between spray-drying parameters, microcapsule structure, and coating performance. The results are expected to provide new insights into the design of environmentally friendly self-healing coatings and offer a feasible strategy for improving the durability of bamboo-based materials.

## 2. Materials and Methods

### 2.1. Experimental Materials

The materials used for the preparation of microcapsules are listed in Table 1. Chitosan (acetylation degree: 80.0%~95.0%, molecular weight: 150,000 g/mol) was used as the shell material. The average air-dried density of bamboo board was about 0.70 g/$cm^3$, and the moisture content was conditioned to 5.0 ± 1.0% under controlled conditions (25 °C, 60% RH) 14 days before coating.

**Table 1.** List of chemicals and materials in the test.

| Material Name | Specification/Dimension | Place of Origin |
|---|---|---|
| Chitosan | Analytically pure | Sinopharm Chemical Reagent Co., Ltd., Beijing, China |
| Acetic acid | Analytically pure | Sinopharm Chemical Reagent Co., Ltd., Beijing, China |

**Table 1.** *Cont.*

| Material Name | Specification/Dimension | Place of Origin |
| --- | --- | --- |
| Gum arabic powder | Analytically pure | Tianjin Zhonglian Chemical Reagent Co., Ltd., Tianjin, China |
| Tween-80 (emulsifier) | Analytically pure | Shandong Yousuo Chemical Technology Co., Ltd., Linyi, China |
| Polymerized tung oil | | Gushi Anshan Tung Oil Sales Co., Ltd., Xinyang, China |
| Bamboo boards | 100 mm × 50 mm × 5 mm | Zhejiang Qingyuan Huachuang Bamboo Co., Ltd., Lishui, Zhejiang, China |

### 2.2. Preparation of TO/CS-GA MCs

As shown in Figure 1, a heat-collecting constant-temperature magnetic stirrer (DF-101Z, Shanghai Yixin Scientific Instrument Co., Ltd., Shanghai, China) was used in the preparation process. First, 1.0 g of chitosan was dissolved in 100 mL of a 2.0% acetic acid solution (2.0 mL acetic acid added to 98.0 mL deionized water) and stirred at 50 °C and 1000 rpm for 30 min to obtain the chitosan solution. Subsequently, 5.0 g of gum arabic powder was added to 100.0 mL of deionized water and stirred at 50 °C and 1000 rpm for 5 min until completely dissolved to obtain the gum arabic solution. Then, 3.0 g of tung oil and 0.30 g of Tween-80 were added to the gum arabic solution and stirred at 50 °C and 1000 rpm for 2 h. An ultrasonic emulsifying disperser (BILONG-500, Shanghai Bilang Instrument Co., Ltd., Shanghai, China) was then used to emulsify the mixture for 10 min to prepare the core emulsion. Afterward, the chitosan solution was added dropwise to the core emulsion, and the pH was adjusted to approximately 3.5 using 1 mol $L^{-1}$ hydrochloric acid. The reaction was carried out at 50 °C and 1000 rpm for 60 min. After cooling, the mixture was allowed to stand for 6 h. Subsequently, deionized water was added for dilution at a ratio of 1:1. Finally, two types of TO/CS–GA MCs were obtained using a small spray dryer (JA-PWGZ100, Shenyang Jingao Instrument Technology Co., Ltd., Shenyang, China) at feed rates of 100 and 200 mL $h^{-1}$, respectively, with an outlet temperature of 110 °C. The microcapsules prepared at a feed rate of 100 mL $h^{-1}$ were labeled as microcapsules 1#, while those prepared at a feed rate of 200 mL $h^{-1}$ were labeled as microcapsules 2#.

### 2.3. Preparation of TO/CS-GA MCs Self-Healing Coatings

As shown in Table 2, the bamboo board was polished with 1000-mesh sandpaper to make it smooth, and then 0.25 g of tung oil was evenly coated on the polished bamboo board surface and placed in an oven (DHG-9240A, Shanghai Aozhen Instrument Manufacturing Co., Ltd., Shanghai, China) at 50 °C. After drying for 24 h, it was taken out and polished with 1000 grit sandpaper to make it smooth, repeated the above experimental operation again, and then 0.50 g of the coating prepared by adding the two microcapsules to tung oil in ratios of 0 wt%, 1.0 wt%, 3.0 wt%, 5.0 wt%, 7.0 wt%, 9.0 wt%, and 11.0 wt% was evenly applied to the surface of the polished bamboo board. After drying in an oven at 50 °C for 72 h, it was taken out and polished with 1000 grit sandpaper to make it smooth, repeated the above coating, drying and polishing operations once to obtain microcapsule coatings on the bamboo surface. The coating amount of each bamboo board surface was 1.00 g, and the coating amount was about 200.00 g/$m^2$. Microcapsules 1# were added to tung oil in proportions of 0 wt%, 1.0 wt%, 3.0 wt%, 5.0 wt%, 7.0 wt%, 9.0 wt% and 11.0 wt%, respectively. The prepared coatings were named 0, 1-1, 1-2, 1-3, 1-4, 1-5 and 1-6 in sequence. Similarly, microcapsules 2# were added to tung oil at ratios of 1.0 wt%, 3.0 wt%, 5.0 wt%, 7.0 wt%, 9.0 wt% and 11.0 wt%, and the resulting coatings were numbered as 2-1, 2-2, 2-3, 2-4, 2-5 and 2-6 respectively.

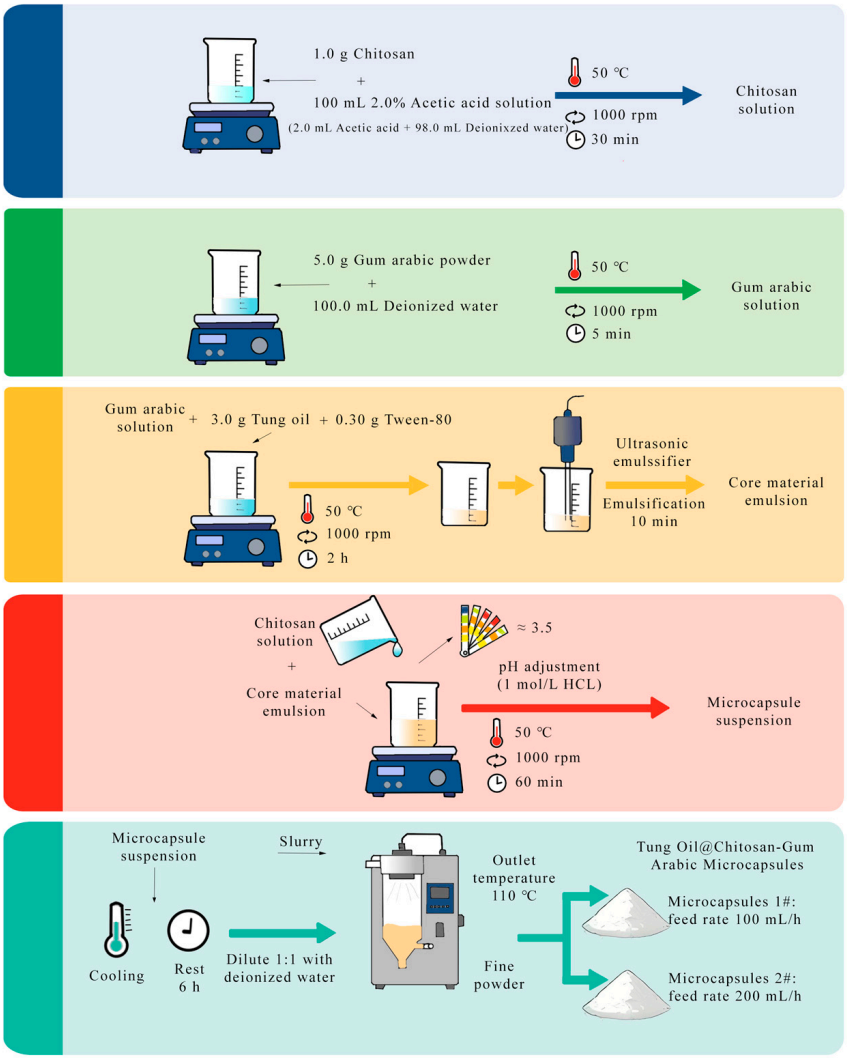


**Figure 1.** Schematic diagram of the preparation process of TO/CS–GA MCs.

**Table 2.** Microcapsules content in bamboo coatings.

| Coating Number | Microcapsules Proportion (wt%) | Tung Oil Content (g) | Microcapsules Mass (g) | Total Amount of Coating (g) |
|---|---|---|---|---|
| 0 | 0 | 1.00 | 0 | 1.00 |
| 1-1 | 1.0 | 0.99 | 0.01 | 1.00 |
| 1-2 | 3.0 | 0.97 | 0.03 | 1.00 |
| 1-3 | 5.0 | 0.95 | 0.05 | 1.00 |
| 1-4 | 7.0 | 0.93 | 0.07 | 1.00 |
| 1-5 | 9.0 | 0.91 | 0.09 | 1.00 |
| 1-6 | 11.0 | 0.89 | 0.11 | 1.00 |
| 2-1 | 1.0 | 0.99 | 0.01 | 1.00 |
| 2-2 | 3.0 | 0.97 | 0.03 | 1.00 |
| 2-3 | 5.0 | 0.95 | 0.05 | 1.00 |
| 2-4 | 7.0 | 0.93 | 0.07 | 1.00 |
| 2-5 | 9.0 | 0.91 | 0.09 | 1.00 |
| 2-6 | 11.0 | 0.89 | 0.11 | 1.00 |

### *2.4. Testing and Characterization*

#### 2.4.1. Micromorphological Characterization

The surface morphology and particle size distribution of the microcapsules were observed by scanning electron microscopy (SEM) (QUANTA-200, Thermo Fisher Scientific, Waltham, MA, USA), and the healing effect of the self-healing coatings prepared by microcapsules was observed under an optical microscope (AX-10, Carl Zeiss AG, Oberkochen, Germany).

#### 2.4.2. Chemical Composition

The chemical composition of the microcapsules and coatings was tested and characterized by using a Fourier transform infrared spectrometer (FTIR) VERTEX80V, Bruker Technology Co., Ltd., Ettlingen, Germany. Before testing the coating samples, the surface of the attenuated total reflectance (ATR) crystal, a circular disk with a diameter of 3 mm fabricated from diamond, was cleaned. The coating samples were then cut to an appropriate size for measurement. The sample was placed to be tested on the surface of an ATR crystal. For FTIR analysis of the microcapsules, the KBr pellet method was used in transmission mode. In contrast, ATR mode was employed only for the coating samples. Approximately 1 mg of sample was mixed with 100 mg of KBr powder and pressed into pellets using a tablet press under a pressure of 10 MPa for 1 min.

#### 2.4.3. Microcapsule Encapsulation Efficiency Test

The 1.0 g of microcapsule powder was weighed and ground into a fine powder. The ethanol was added to completely soak the microcapsule powder for 24 h. Then, a vacuum filter (SHZ-D, Shanghai Smart Instrument Equipment Co., Ltd., Shanghai, China) was used to perform suction filtration. After drying, the shell material of microcapsules was obtained. $m_1$ was the weighed mass of microcapsules, $m_2$ was the weighed mass of shell material, and the encapsulation efficiency was $P$. The encapsulation efficiency of the microcapsules (Equation (1)) was calculated. The experimental data were tested 5 times, and the average value was taken.

$$P = \frac{m_1 - m_2}{m_1} \times 100\% \quad (1)$$

#### 2.4.4. Optical Performance Testing

Color difference test method: According to GB/T 11186-2025, "Methods for measuring the color of coatings" [30], a portable colorimeter (CR7, Shenzhen Sanenshi Technology Co., Ltd., Shenzhen, China) was used to test the color difference in the coatings. Each coating was tested 5 times, and the average value was calculated and recorded as $L$, $a$ and $b$ values. The $L$ value represents the lightness and darkness value of the measured sample. The larger the $L$ value, the brighter the color. The $a$ value represents the red-green value. A positive $a$ value represents a reddish color, and a negative $a$ value represents a greenish color. The $b$ value represents the yellow-blue value. A positive $b$ value means the color is yellowish, and a negative $b$ value means the color is bluish. The test values of the coatings without microcapsules were $L_1$, $a_1$, $b_1$, and the test values of the coatings with microcapsules were $L_2$, $a_2$, $b_2$. The color difference $\Delta E$ was calculated according to Equation (2). Among them, $\Delta L = L_2 - L_1$, $\Delta a = a_2 - a_1$, $\Delta b = b_2 - b_1$.

$$\Delta E = \left[ (\Delta L)^2 + (\Delta a)^2 + (\Delta b)^2 \right]^{\frac{1}{2}} \quad (2)$$

Gloss test method: According to GB/T4893.6-2013, "Test of surface coatings of furniture—Part 6: Determination of gloss value" [31], a gloss meter (HG268, Shenzhen

Sanenshi Technology Co., Ltd.) was used to measure the gloss of the coatings at incident angles of 20°, 60° and 85°.

#### 2.4.5. Mechanical Performance Testing

Hardness test method: A pencil was used to measure the hardness of the coatings according to the standard GB/T 6739-2022, "Paints and varnishes—Determination of film hardness by pencil test" [32]. Pencils were placed with a hardness of 6B—6H on the mechanical trolley in sequence. After the placement was completed, the trolley was pushed horizontally so that the pencils on the trolley were evenly applied to the coating. The scratches were observed on the coating. The hardness of the coating was defined as the highest pencil grade that did not cause visible damage to the coating surface.

Impact resistance test method: According to the standard GB/T4893.9-2013, "Test of surface coatings of furniture—Part 9: Determination of resistance to impact" [33], an impact testing machine was used to measure the impact resistance of the coatings. The ball was raised to a specified height, usually from low to high. Then the ball was released, and the impact was observed on the coatings left by the ball. The impact resistance was recorded as the maximum impact value that did not cause visible damage to the coating surface.

Adhesion test method: According to the standard GB/T 4893.4-2023, "Physical and Chemical Performance Test of Furniture Surface Coatings—Part 4: Adhesion Cross-cutting Measurement Method" [34], a knife was used to test the adhesion of the coatings. A multi-blade cutter was held and cut at an angle of approximately 45° to the coating, then the coating was rotated 90° and cut once to form a grid pattern. The grade of coating adhesion was divided into grades 1–5. The smaller the grade, the less the coatings will peel off, and the cutting edge will be smoother. The determination of the coating's adhesion grade is shown in Table 3.

**Table 3.** Coatings adhesion grade determination.

| Classification | Explanation | Surface Appearance of the Cross-Cutting Area That Has Fallen Off (Taking Six Parallel Cutting Lines as an Example) |
|---|---|---|
| 0 | The cutting edge is completely smooth with no peeling off. | -- |
| 1 | There is a small amount of coating peeling off at the cutting intersection, and the affected area of the cross-cutting should not exceed 5%. | 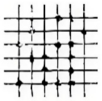 |
| 2 | There is coating peeling at the cutting edge and/or intersection, and the affected cutting area is greater than 5% but less than 15%. |  |
| 3 | The coatings partially or entirely fall off in large fragments along the cutting edge, and/or partially or entirely fall off at different parts of the grid. The affected cutting area is greater than 15% and less than 35%. |  |

**Table 3.** *Cont.*

| Classification | Explanation | Surface Appearance of the Cross-Cutting Area That Has Fallen Off (Taking Six Parallel Cutting Lines as an Example) |
|---|---|---|
| 4 | Large fragments of the coatings fall off along the cutting edge and/or partially or completely fall off in some grids. The affected cutting area is greater than 35% and less than 65%. | 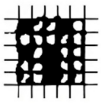 |
| 5 | Any degree of detachment beyond Grade 5. | |

Roughness test method: According to the national standard GB/T1031-2009, "Geometrical Product Specifications (GPS)—Surface Texture: Profile Method Surface Roughness Parameters and their Values" [35], a touch probe precision roughness tester (J84C, Shanghai Taiming Optical Instrument Co., Ltd., Shanghai, China) was used to measure the roughness of the coatings.

#### 2.4.6. Self-Healing Performance Test

The scratch test was used to test the self-healing performance of coatings. A razor blade was used to scratch the surface of the coatings, an optical microscope was used to observe, and the width of the scratch was recorded. At this time, the width of the scratch was recorded ($W_1$). The scratch was observed at this location again after 48 h, and the scratch width was recorded ($W_2$). The self-healing efficiency of coatings ($H$) was calculated by Equation (3).

$$H = \frac{W_1 - W_2}{W_1} \times 100\% \quad (3)$$

#### 2.4.7. Analysis of Variance (ANOVA)

The variance analysis of the experimental data was conducted using non-repetitive two-factor analysis. As a measure of significance, the *p-value* evaluated whether an experimental result could reasonably have occurred by chance. $F$ was the test statistic used when calculating hypothesis testing. *F crit* referred to the threshold of the $F$ statistic determined by a given significance level. Specifically, the threshold for determining statistical significance was defined as $0.01 < p\text{-}value < 0.05$, where $p\text{-}value \leq 0.01$ means the difference was extremely significant, and $p\text{-}value > 0.05$ means the difference was not significant. When $F > F\ crit$, from a statistical point of view, this indicated that the difference between the groups was significant; when $F < F\ crit$, there was no significant difference.

## 3. Results and Discussion

### *3.1. Microcapsules Analysis*

The SEM images and corresponding particle size distribution histograms are shown in Figure 2A,B. From the normal distribution diagram, it can be seen that the particle size of microcapsules 1# is approximately 3.46 ± 2.73 μm, while the particle size of microcapsules 2# is approximately 4.01 ± 2.48 μm.

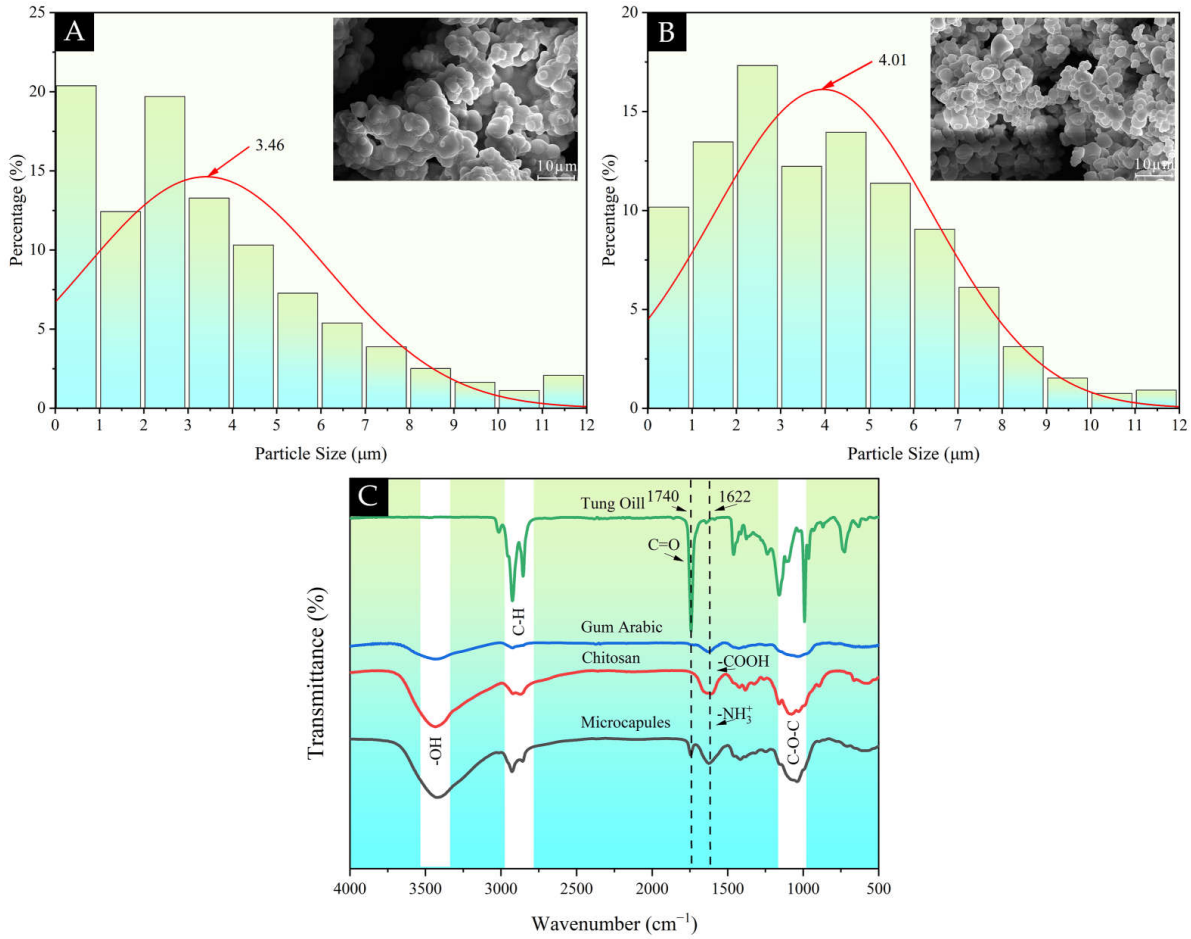


**Figure 2.** (**A**) Microcapsules 1# particle size distribution, (**B**) Microcapsules 2# particle size distribution. The SEM images were obtained at a magnification of 5000×, and the scale bar represented 10 μm. (**C**) FTIR spectra of the microcapsules.

Figure 2C shows the FTIR spectrum of the microcapsules. The characteristic absorption peaks of tung oil at 2926 $cm^{-1}$ (C–H stretching vibration), 1740 $cm^{-1}$ (C=O stretching vibration), and 991 $cm^{-1}$ (conjugated double bond bending vibration) are clearly visible, indicating that the core material tung oil was successfully introduced into the system. The characteristic peaks of chitosan appear at 3415 $cm^{-1}$ (–OH stretching vibration), 1647 $cm^{-1}$ (amide I band) and 1040 $cm^{-1}$ (C–O–C stretching vibration). As a polysaccharide material, gum arabic has its –OH absorption peak near 3500 $cm^{-1}$. In addition, the absorption peak appearing at 1622 $cm^{-1}$ can be attributed to the electrostatic interaction between the –COOH group in gum arabic and the $–NH_3^+$ group of chitosan, further proving the formation of the composite shell material structure.

### *3.2. Microcapsule Encapsulation Efficiency Analysis*

The calculated encapsulation efficiency of microcapsules 1# and microcapsules 2# is shown in Table 4. The results indicate that the encapsulation efficiency of microcapsule 1# is 29.32 ± 2.15%, which is greater than that of microcapsule 2#, which is 26.48 ± 1.83%. The higher the encapsulation efficiency and the higher the core material content, the better the self-healing performance of the microcapsules [36]. Therefore, the self-healing performance of the microcapsules 1# is speculated to be better.

**Table 4.** Determination of microcapsule encapsulation efficiency.

| Types of Microcapsules | $m_1$ (g) | $m_2$ (g) | $p$ (%) |
|---|---|---|---|
| Microcapsules 1# | 1.00 | 0.71 ± 0.02 | 29.32 ± 2.15 |
| Microcapsules 2# | 1.00 | 0.74 ± 0.02 | 26.48 ± 1.83 |

### *3.3. Coating Surface Morphology Analysis*

As shown in Figure 3, as the microcapsule content increases, the surface morphology of the coatings changes significantly. When the content of microcapsules was less than 7.0 wt%, as shown in Figure 3B, the microcapsules can be relatively evenly embedded in the coatings, with only a small amount of particle accumulation, and the uniformity and integrity of the coatings can still be maintained. However, when the microcapsule content further increases, as shown in Figure 3C, a large number of microcapsules are obviously agglomerated on the surface, forming an irregular accumulation of particles, resulting in a significantly enhanced uneven distribution of coatings.

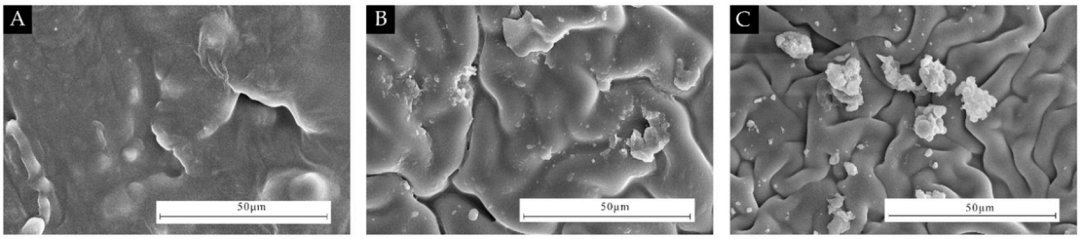


**Figure 3.** SEM images of coatings: (**A**) Coating without microcapsules, (**B**) Coating with 5.0 wt% microcapsules 1#, (**C**) Coating with 11.0 wt% microcapsules 1#.

### *3.4. Analysis of Optical Performance of Coatings*

As shown in Figure 4A,B, when the microcapsule content increased to 11.0 wt%, the gloss at a 60° incident angle of the coatings prepared with microcapsules 1# decreased from 7.12 GU to 1.64 GU, while that of the coatings prepared with microcapsules 2# decreased from 7.12 GU to 1.44 GU. Overall, the gloss of the coatings gradually decreased with increasing microcapsule content. Under the same addition amount, the gloss of the coatings containing microcapsules 1# was generally higher than that of the coatings containing microcapsules 2#. The incorporation of microcapsules alters the surface micromorphology and light scattering behavior of the coating. As the microcapsule content increases, the number of heterogeneous interfaces within the coating matrix also increases. Consequently, incident light undergoes multiple scattering at these interfaces, resulting in a significant reduction in gloss at a 60° incident angle. A similar phenomenon has been reported in previous studies on microcapsule-modified coatings. Deng et al. found that the addition of tung oil microcapsules into UV coatings led to a noticeable decrease in gloss due to the increased surface roughness and enhanced diffuse reflection caused by solid particles dispersed in the coating matrix [20]. In their study, the gloss of the UV coating film decreased after incorporating microcapsules compared with the blank coating, indicating that the presence of microcapsules significantly affects the optical properties of coatings. As shown in Figure 4C, the color difference ($\Delta E$) gradually increased with increasing microcapsule content. Under the same addition amount, the $\Delta E$ value of coatings prepared with microcapsules 1# was generally higher than that of coatings prepared with microcapsules 2#. Compared with microcapsules 2#, microcapsules 1# exhibited better gloss retention but caused a more pronounced increase in color difference. This phenomenon can be attributed to the optical characteristics of the microcapsule shell material. The chitosan—gum arabic

shell exhibits a milky-white appearance, and the dispersion of microcapsules within the coating disrupts the refractive index matching of the coating matrix, thereby reducing the optical uniformity of the coating surface and leading to an increase in $\Delta E$ with increasing microcapsule content. For the microcapsules prepared at a feed rate of 100 mL $h^{-1}$, the particle size was smaller, and the size distribution was more concentrated, resulting in a more uniform coating structure and weaker light scattering effects. Therefore, at the same addition ratio, coatings containing microcapsules prepared at 100 mL $h^{-1}$ exhibited better gloss retention. These results indicate that microcapsule incorporation inevitably influences the optical appearance of coatings, and an appropriate microcapsule content is necessary to balance self-healing functionality and surface optical performance.

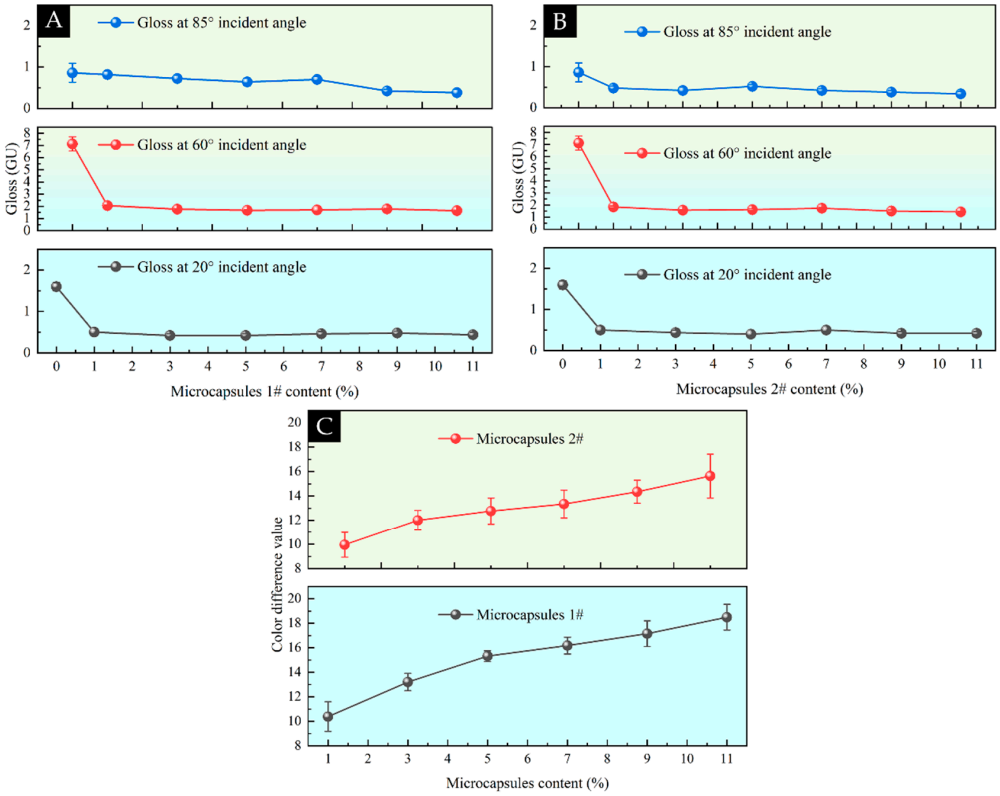


**Figure 4.** (**A**) Changes in coatings gloss with added microcapsules 1#, (**B**) Changes in coatings gloss with added microcapsules 2#, (**C**) Changes in color difference value of coatings. Error bars represent standard deviation (n = 5).

As shown in Table 5, the *p-value* of the microcapsules content is 0.0424 < 0.05 and *F* (5.4957) > *F crit* (5.0503), which indicates that the microcapsule content has a significant impact on the gloss at an incident angle of 60°; the *p-value* of the microcapsules type is 0.0263 < 0.05, and *F* (9.7262) > *F crit* (6.6079), indicating that the microcapsules type also has a significant impact on the gloss at an incident angle of 60°. Therefore, a lower microcapsule content and a lower feed rate can better maintain the gloss of the coating surface.

As shown in Table 6, the *p-value* of the microcapsule content is 0.0021 < 0.05, and *F* is 21.8311 > *F crit* is 5.0503, which indicates that the microcapsules content has a significant impact on color difference; the *p-value* of the microcapsules type is 0.0042 < 0.05, and *F* is 24.7154 > *F crit* is 6.6079, indicating that the microcapsules type also has a significant impact on color difference. Therefore, a lower microcapsule content and a higher feed rate can effectively reduce color difference.

**Table 5.** Analysis of the significance of 60° incident angle gloss by adding different types of microcapsules at different concentrations.

| *Difference Source* | *SS* | *df* | *MS* | *F* | *p-Value* | *F Crit* |
|---|---|---|---|---|---|---|
| Content of microcapsules | 0.1907 | 5.0000 | 0.0381 | 5.4957 | 0.0424 | 5.0503 |
| Types of microcapsules | 0.0675 | 1.0000 | 0.0675 | 9.7262 | 0.0263 | 6.6079 |
| Error | 0.0347 | 5.0000 | 0.0069 | | | |
| Total | 0.2929 | 11.0000 | | | | |

Note: "content of microcapsules" refers to the added content ranging from 1 to 11 wt%, while "types of microcapsules" refers to microcapsules prepared under different spray-drying feed rates (100 and 200 mL $h^{-1}$).

**Table 6.** Analysis of the significance of color difference in coatings by adding different types of microcapsules at different concentrations.

| *Difference Source* | *SS* | *df* | *MS* | *F* | *p-Value* | *F Crit* |
|---|---|---|---|---|---|---|
| Content of microcapsules | 59.3023 | 5.0000 | 11.8605 | 21.8311 | 0.0021 | 5.0503 |
| Types of microcapsules | 13.4274 | 1.0000 | 13.4274 | 24.7154 | 0.0042 | 6.6079 |
| Error | 2.7164 | 5.0000 | 0.5433 | | | |
| Total | 75.4461 | 11.0000 | | | | |

Note: "content of microcapsules" refers to the added content ranging from 1 to 11 wt%, while "types of microcapsules" refers to microcapsules prepared under different spray-drying feed rates (100 and 200 mL $h^{-1}$).

### *3.5. Analysis of Mechanical Performance of Coatings*

As shown in Figure 5, as the amount of microcapsules increases, the hardness, impact resistance, and adhesion grade of the coatings exhibit a trend of first increasing and then decreasing. As the content of microcapsules increased to 11.0 wt%, the hardness of the coatings prepared by microcapsule 1# increased from HB to 2H and then decreased to HB, reaching the maximum value of 2H when the content of microcapsules was 5.0 wt%. The hardness of the coatings prepared by microcapsules 2# increased from HB to H and then decreased back to HB, reaching the maximum value of 2H when the microcapsule content was 3.0–5.0 wt%. With the increase in microcapsule content to 11.0 wt%, the impact resistance of the coatings prepared by microcapsule 1# increased from 2 kg·cm to 4 kg·cm and then decreased to 2 kg·cm, reaching the maximum value of 4 kg·cm when the microcapsule content was 7 wt%. The impact resistance of the coatings prepared by microcapsules 2# increased from 2 kg·cm to 3 kg·cm, reaching the maximum value of 3 kg·cm when the content of microcapsules was more than 5.0 wt%. As the content of microcapsules increased to 11.0 wt%, the adhesion grade of the coatings prepared by microcapsule 1# increased from 2 to 3 and then decreased to 1, reaching the highest grade of 3 when the content of microcapsules was 3.0–5.0 wt%. The adhesion grade of the coatings prepared by microcapsules 2# increased from 1 to 2 and then decreased to 1, reaching the highest grade 2 when the microcapsule content was 5.0–9.0 wt%. As the microcapsule content increased to 11.0 wt%, the roughness of the coatings prepared by microcapsule 1# increased from 2.24 ± 0.81 μm to 11.97 ± 0.38 μm. The roughness of the coatings prepared by microcapsules 2# increased from 3.33 ± 0.51 μm to 7.93 ± 0.72 μm; in most of the 1.0–9.0 wt% addition intervals, the roughness of the coatings containing microcapsules 1# is lower than that of the coatings containing microcapsules 2#. Microcapsules 1# are more effective in improving the hardness, impact resistance, and surface smoothness of the coatings. When the microcapsule content increased from 1.0 wt% to 5.0 wt%, the microcapsules were uniformly dispersed in the coating matrix and effectively filled the micropores and defects. This filling effect improved the compactness of the coating and strengthened the interfacial bonding within the coating

structure. Thereby enhancing the hardness and impact resistance of the coatings. However, when the microcapsule content exceeded 7.0 wt%, obvious agglomeration of microcapsules occurred in the coating matrix. The excessive aggregation of microcapsules weakened the local interfacial bonding and led to stress concentration within the coating, which ultimately resulted in the deterioration of mechanical properties. Similar phenomena have also been reported in previous studies on microcapsule-modified coatings. Deng et al. reported that moderate microcapsule content can improve the compactness and mechanical performance of coatings, while excessive microcapsule loading tends to cause particle agglomeration and structural defects, leading to reduced coating mechanical strength [20]. This behavior indicates that a better microcapsule content is necessary to balance reinforcement and structural stability in microcapsule-based self-healing coatings. These structural defects may act as crack initiation sites under external loading, resulting in a decrease in hardness and impact resistance. When a small number of microcapsules is introduced, some particles are distributed near the coating-substrate interface, which partially interrupts the direct contact between the tung oil matrix and the bamboo substrate. This weakens the mechanical interlocking and interfacial bonding, resulting in a temporary decrease in adhesion performance. As the microcapsule content further increases, the particles can fill the microvoids and defect structures within the coating layer, improving the compactness of the coating and enhancing the mechanical interlocking with the substrate. Consequently, the adhesion performance improves, and the adhesion grade decreases. The roughness increases with the addition amount, mainly because some microcapsules are distributed near the surface of the coatings and even partially exposed on the surface, forming micro-scale convex structures, thereby increasing the unevenness of the surface morphology. Under the same addition ratio, the microcapsules prepared under 100 mL $h^{-1}$ conditions have a smaller average particle size and a higher encapsulation efficiency. The smaller particle size is beneficial to the uniform dispersion of microcapsules in the coatings, reducing the degree of damage to the continuous phase structure and weakening the stress concentration effect. Therefore, the coatings in this system showed better mechanical performance, with a maximum hardness of up to 2H and an impact resistance of 4 kg·cm.

As shown in Table 7, the *p-value* of microcapsules content is 0.0263 < 0.05 and *F* is 6.9736 > *F crit* is 5.0503, which indicates that the microcapsules content has a significant impact on roughness; the *p-value* of microcapsules type is 0.7363 > 0.05 and *F* is 0.1268 < *F crit* is 6.6079, which indicates that the impact of microcapsules type on roughness is not significant. Therefore, a lower microcapsule content can better reduce the increase in the surface roughness of the coatings.

**Table 7.** Analysis of the significance of the roughness of coatings by adding different types of microcapsules at different concentrations.

| *DifferenceSource* | *SS* | *df* | *MS* | *F* | *p-Value* | *F Crit* |
|---|---|---|---|---|---|---|
| Content of microcapsules | 63.4073 | 5.0000 | 12.6815 | 6.9736 | 0.0263 | 5.0503 |
| Types of microcapsules | 0.2305 | 1.0000 | 0.2305 | 0.1268 | 0.7363 | 6.6079 |
| Error | 9.0925 | 5.0000 | 1.8185 | | | |
| Total | 72.7303 | 11.0000 | | | | |

Note: "Content of microcapsules" refers to the added content ranging from 1 to 11 wt%, while "types of microcapsules" refers to microcapsules prepared under different spray-drying feed rates (100 and 200 mL $h^{-1}$).

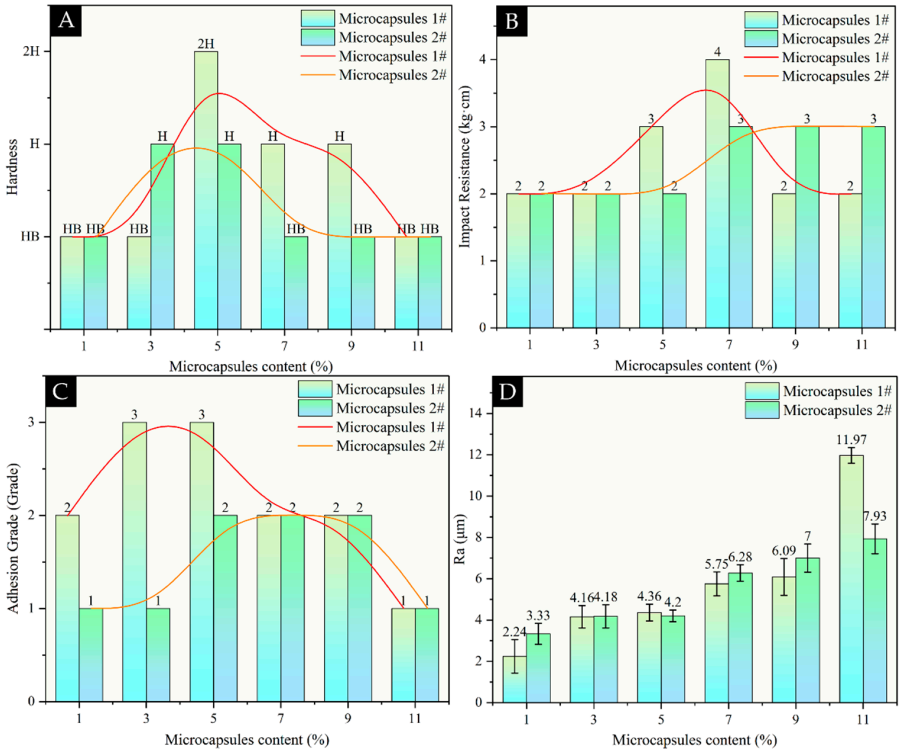


**Figure 5.** (**A**) Changes in coating hardness, (**B**) Changes in coating impact resistance, (**C**) Changes in coating adhesion grade, (**D**) Changes in coating roughness. Error bars represent standard deviation (n = 5).

### *3.6. Analysis of Self-Healing Performance of Bamboo Substrate Coatings*

Artificial scratches were created on the coating surface using a razor blade, and the healing effect was observed under a microscope for 48 h at room temperature, as shown in Figure 6. As shown in Figure 6(A1,A2), the width of scratches on the coating without microcapsules has almost no healing effect. However, when 5.0 wt% microcapsules were added, the width of the coating scratches decreased from 22.20 ± 0.29 μm to 16.10 ± 0.25 μm and from 26.49 ± 0.42 μm to 21.54 ± 0.52 μm, as shown in Figure 6(D1,D2,K1,K2). As shown in Figure 6(F1,F2,L1,L2), the width of the coating scratches decreased from 34.00 ± 0.32 μm to 26.91 ± 0.43 μm, and from 53.96 ± 1.30 μm to 47.53 ± 0.85 μm, respectively. When the microcapsule content exceeded 7.0 wt%, the self-healing efficiency of the coatings began to decrease. Therefore, the microcapsule content of 5.0–7.0 wt% had a better scratch healing effect.

The self-healing efficiency of coatings is shown in Figure 7. Within 48 h after the damage occurs, as the microcapsules in the coatings rupture under the action of external force, the core material is rapidly released and penetrated into the scratched area, and the scratches begin to be gradually filled and healed. As the content of microcapsules increased to 11.0 wt%, the self-healing efficiency of the coatings prepared by microcapsule 1# increased from 9.54 ± 0.24% to 28.16 ± 0.63% and then decreased to 14.83 ± 0.46%, reaching the maximum value of 28.16 ± 0.63% when the content of microcapsules was 5.0 wt%. The self-healing efficiency of the coatings prepared by microcapsule 2# increased from 9.28 ± 0.25% to 18.44 ± 0.43% and then decreased to 9.37 ± 0.21%, reaching the maximum value of 18.44 ± 0.43% when the microcapsule content was 7.0 wt%. When the addition amounts of microcapsules were 5.0–7.0 wt%, the self-healing efficiency reached the peak after 48 h; when the added amount exceeded 7.0 wt%, the self-healing efficiency decreased. Under the same addition ratio, the self-healing efficiency of the coatings con-

taining microcapsules 1# is higher than that of microcapsules 2#. Comprehensive results show that the coatings containing microcapsule 1# show better self-healing performance.

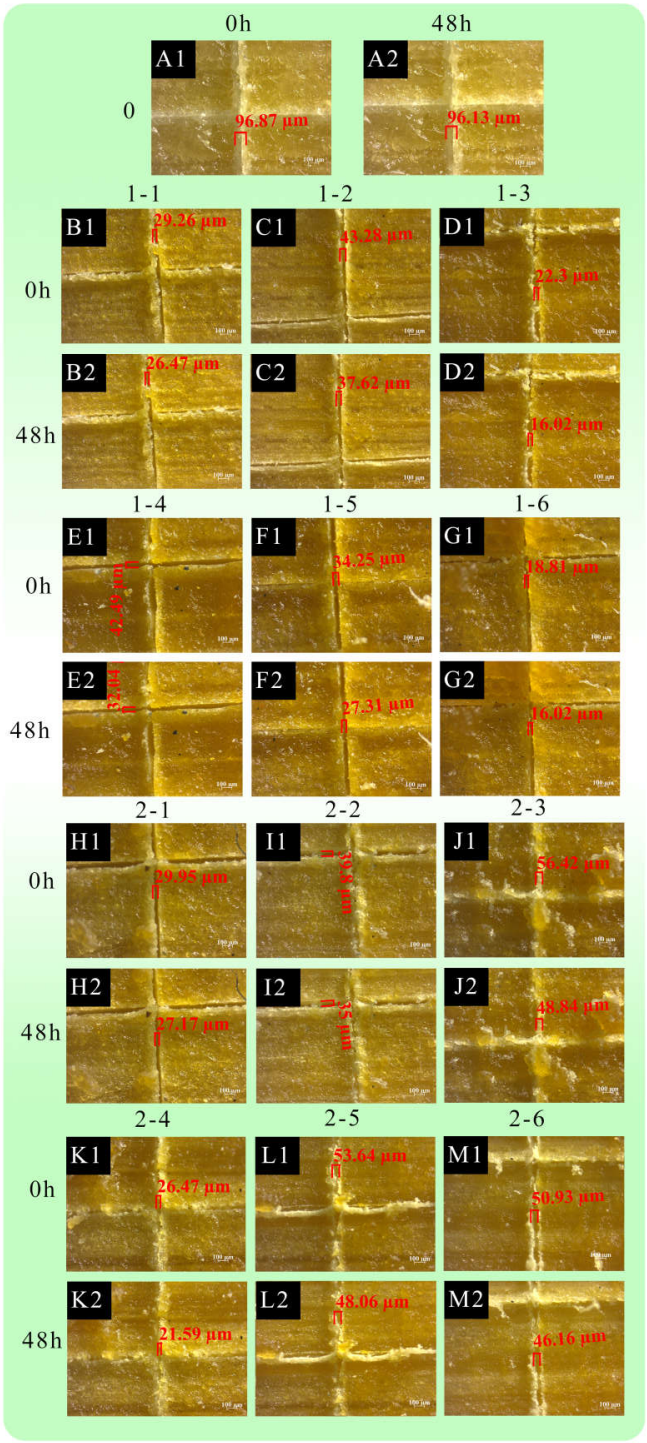


**Figure 6.** Self-healing behavior of bamboo coatings. (**A1**,**A2**) The scratch width of sample 0 before healing and after 48 h, (**B1**–**G2**) The width scratch of samples 1-1, 1-2, 1-3, 1-4, 1-5, 1-6 before healing and after 48 h, (**H1**–**M2**) The width scratch of samples 2-1, 2-2, 2-3, 2-4, 2-5, 2-6 before healing and after 48 h. The image selection criterion is to choose the image with the smallest deviation from the average scratch width as the reference.

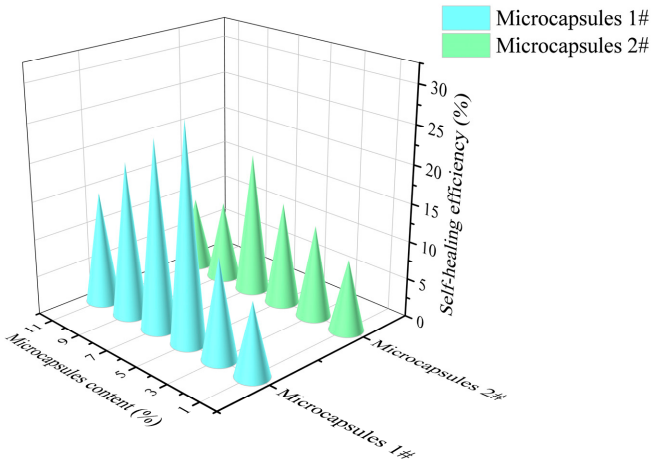


**Figure 7.** Changes in the coating's self-healing efficiency.

The self-healing mechanism of the microcapsule coatings is shown in Figure 8. The TO/CS-GA MCs are evenly distributed in the tung oil and coated on the surface of the bamboo. When the coatings were subject to external force or damage, the internal microcapsules ruptured and released the core material, tung oil. This exposes the core to scratches, and the air then acts on the core, allowing it to solidify the tung oil and repair the coatings. When the microcapsule content increases from 1.0 wt% to 7.0 wt%, the number of microcapsules that can be effectively broken in the coatings increases, and the released tung oil core material can fully penetrate and fill the scratched area, and then form a continuous and dense repair film layer through oxidative polymerization reaction. The self-healing process in this study was conducted at room temperature. Since the viscosity of tung oil is temperature-dependent, higher temperatures may accelerate the flow and oxidative polymerization of the released oil, potentially enhancing the healing efficiency. When the addition amount exceeds 7.0 wt%, the microcapsules agglomerate in the coatings and interface defects increase, making it difficult for some microcapsules to effectively break or be blocked in release during the damage process. At the same time, the high filling amount weakens the overall structural integrity of the coatings, causing the continuity of the film formation in the healing area to decrease, ultimately leading to a reduction in self-healing efficiency.

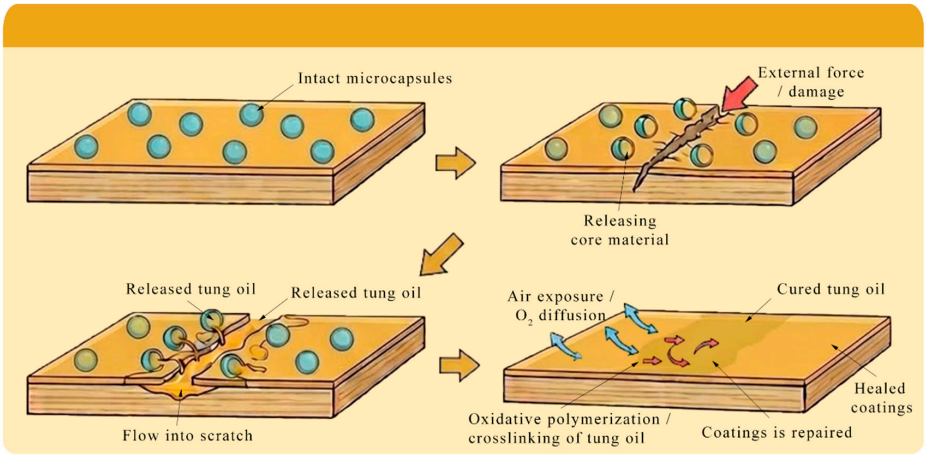


**Figure 8.** Self-healing mechanism of microcapsule coatings.

In addition, the encapsulation efficiency of microcapsules prepared under 100 mL $h^{-1}$ conditions is 29.32 ± 2.15%, which is higher than that of the 200 mL $h^{-1}$ sample, indicating

that its core material content is higher and the reserves of effective healing components are more sufficient. Therefore, at a 5.0 wt% addition ratio, the self-healing efficiency of the coatings reaches 28.16 ± 0.63%, which is significantly better than the coatings prepared with a high feed rate. The maximum self-healing efficiency (28.16 ± 0.63%) is comparable to previously reported microcapsule-based wood coatings. For instance, Dong et al. reported healing efficiencies of approximately 20%–25% in tung oil microcapsule coatings on wood surfaces [27]. Similarly, other self-healing coating systems based on vegetable oils have demonstrated healing efficiencies ranging from 15% to 30%, depending on microcapsule content and shell structure [29].

As shown in Table 8, the *p-value* of microcapsules content is 0.1103 > 0.05 and *F* is 3.2588 < *F crit* is 5.0503, indicating that the effect of microcapsules content on self-healing efficiency is not significant; the *p-value* of microcapsules type is 0.0378 < 0.05 and *F* is 7.8652 > *F crit* is 6.6079, indicating that microcapsules type has a significant impact on self-healing efficiency. Therefore, the coatings prepared by microcapsules with a lower feed rate have better self-healing performance.

**Table 8.** Analysis of the significance of the self-healing efficiency of coatings by adding different types of microcapsules at different concentrations.

| *DifferenceSource* | *SS* | *df* | *MS* | *F* | *p-Value* | *F Crit* |
|---|---|---|---|---|---|---|
| Content of microcapsules | 0.0243 | 5.0000 | 0.0049 | 3.2588 | 0.1103 | 5.0503 |
| Types of microcapsules | 0.0117 | 1.0000 | 0.0117 | 7.8652 | 0.0378 | 6.6079 |
| Error | 0.0074 | 5.0000 | 0.0015 | | | |
| Total | 0.0434 | 11.0000 | | | | |

Note: "Content of microcapsules" refers to the added content ranging from 1 to 11 wt%, while "types of microcapsules" refers to microcapsules prepared under different spray-drying feed rates (100 and 200 mL $h^{-1}$).

### *3.7. Comprehensive Performance Analysis of Better Samples*

The particle size of microcapsules 1# is smaller than that of microcapsules 2#. The smaller particles help to reduce damage to the coatings [28]. Comprehensive performance analysis shows that the gloss, hardness, impact resistance, roughness and self-healing performance of the coatings added with microcapsules 1# are better than those of the coatings added with microcapsules 2#. The self-healing efficiency of the coatings with added microcapsules 1# reaches its peak when the microcapsule content is 5.0 wt%, and that of the coatings with added microcapsules 2# reaches its peak when the microcapsule content is 7.0 wt%. Lower microcapsule content provides better optical and mechanical performance, so the coatings with microcapsules 1# added and the content at 5.0 wt% is the better sample in this experiment.

From an industrial perspective [37], the materials used in this study, including tung oil, chitosan, and gum arabic, are relatively low-cost and widely available natural materials. Although the preparation of microcapsules introduces additional processing steps such as spray drying, the better added content identified in this work is only 5 wt%, which reduces the overall material cost. Therefore, the proposed coating system shows potential for practical applications in bamboo furniture and decorative materials.

## 4. Conclusions

In this study, TO/CS–GA MCs were successfully prepared by a spray-drying method, and their effects on the performance of bamboo surface coatings were systematically investigated. Two representative spray-drying feed rates (100 and 200 mL $h^{-1}$) were selected to evaluate their influence on the structure and performance of the prepared microcap-

sules as well as the performance of the resulting coatings. Both the content and types of microcapsules significantly affected the optical, mechanical, and self-healing performance of the coatings. With increasing microcapsule content, the gloss of the coatings gradually decreased, and the surface roughness increased, indicating that the incorporation of microcapsules altered the surface microstructure and light-scattering behavior of the coating. In contrast, the mechanical performance and self-healing efficiency of the coatings exhibited a trend of first increasing and then decreasing with increasing microcapsule content. The better microcapsule content was found within the range of 5.0–7.0 wt%, where the coatings achieved a balanced combination of mechanical performance and self-healing capability. In particular, microcapsules 1# prepared at a feed rate of 100 mL $h^{-1}$ exhibited smaller particle sizes and better dispersion within the coating matrix, resulting in improved mechanical performance and enhanced self-healing efficiency. Under the better condition of 5.0 wt% addition, the coating exhibited a hardness of 2H, an impact resistance of 3 kg·cm, and a self-healing efficiency of 28.16 ± 0.63%. Overall, the results demonstrate that the spray-drying feed rate plays a key role in controlling the structure and performance of TO/CS–GA MCs, which in turn significantly influences the performance of bamboo surface coatings. These findings provide useful insights into the development of environmentally friendly self-healing coatings for bamboo materials and offer a feasible strategy for improving the durability of bamboo-based products. Future studies may further explore a wider range of spray-drying parameters to optimize microcapsule preparation and coating performance.

**Author Contributions:** Conceptualization and methodology, writing—review and editing, X.L.; validation, resources, data management, J.H.; resources, H.Y.; formal analysis, J.L.; investigation and supervision, X.Y. All authors have read and agreed to the published version of the manuscript.

**Funding:** This project was partly supported by the Innovation and Entrepreneurship Training Program for College Students in Jiangsu Province (202510298082Z) and the Natural Science Foundation of Jiangsu Province (BK20201386).

**Institutional Review Board Statement:** Not applicable.

**Informed Consent Statement:** Not applicable.

**Data Availability Statement:** Data are contained within the article.

**Conflicts of Interest:** The authors declare that there are no conflicts of interest.

## References

1. Su, J.C.; Chen, Z.Y.; Le, L.; Liu, M.L.; Li, C.F. An overview of the multifunctional research progress and sustainable development trends in bamboo-based composites. *Sustain. Mater. Technol.* **2025**, *46*, e01665. [CrossRef]
2. Wang, H.L.; Jiang, B.S. Research on the Mechanical Performance of Fiber-Reinforced Bamboo Board and Numerical Simulation Analysis of the Structural Mechanical Performance of Products. *Appl. Sci.* **2025**, *15*, 5288. [CrossRef]
3. Lv, Y.; Wei, J.; Huang, Z.; Zhang, Z.; Ding, S.C.; Zhang, C.X.; Wang, W.F.; Xu, K.K.; Xu, R.M.; Wang, L.Y.; et al. Engineered Bamboo Building Materials: Types, Production, and Applications. *Chem. Eng. J.* **2024**, *488*, 151053. [CrossRef]
4. Zhang, Y.; Amin, K.; Zhang, Q.; Yu, Z.Y.; Jing, W.D.; Wang, Z.H.; Lyu, B.; Yu, H.S. The application of dietary fibre as microcapsule wall material in food processing. *Food Chem. Adv.* **2025**, *463*, 141195. [CrossRef]
5. He, H.; An, F.P.; Li, C.N.; Dong, Q.F.; Huang, Q.; Wang, J.Q.; Song, H.B.; Geng, F. Comparative study on the passion fruit essential oil microcapsules constructed from hydrophobic cellulose I/II nanocrystals and gelatin: Physicochemical and release performance. *Food Hydrocoll.* **2026**, *175*, 112479. [CrossRef]
6. Deng, W.F.; Zhang, Y.D.; Toivakka, M.; Xu, C.L. Microencapsulation of phase change materials via nanopolysaccharide complex-stabilized Pickering emulsions. *Carbohydr. Polym.* **2026**, *380*, 125066. [CrossRef]
7. Zhu, J.Y.; Tang, Y.Z.; Zhou, J.; Yang, Z.Z.; He, J.Y.; Zhang, J. Life cycle analysis for reconstituted decorative lumber from an ecological perspective: A Review. *Colloids Surf. A Physicochem. Eng. Asp.* **2026**, *736*, 139611. [CrossRef]
8. Li, W.H.; Sheng, W.; Tian, Y.H.; Guo, H.Z.; Hou, Z.H.; Shi, S.S. Synthesis and Characterization of Hydrophobic Phase Change Microcapsules with $SiO_2$/PUA Composite Shell. *J. Appl. Polym. Sci.* **2026**, *18*, e70498. [CrossRef]

9. Li, Z.H.; Du, G.; Yang, S.; Lu, X.R.; Zheng, F.L.; Hao, B.; Zhan, P.; Li, G.M.; Zhang, H. Self-Healing Imidazole-Cured Epoxy Using Microencapsulated Epoxy-Amine Chemistry. *Polymers* **2025**, *17*, 2391. [CrossRef]
10. Indiarto, R.; Violcy, R.A.; Rahimah, S.; Subroto, E.; Huda, S.; Sikin, A.M. Effect of shell-material composition on physicochemical performance and bioactive retention of spray-dried mangosteen rind microcapsules. *CyTA J. Food* **2026**, *24*, 2616076. [CrossRef]
11. Vera-Rivera, D.; Neira-Viñas, M.; Formosa, J.; Giro-Paloma, J. Microcapsules with thermal, mechanical, and chemical stability from polystyrene waste to contain phase change materials. *J. Energy Storage* **2026**, *143*, 119744. [CrossRef]
12. Yang, S.J.; Lee, K.H. Spontaneous Hollow Coacervate Transition of Silk Fibroin via Dilution and Its Transition to Microcapsules. *Biomacromolecules* **2025**, *26*, 2513–2528. [CrossRef]
13. Ma, Z.; Lv, W.A.; Xu, H.; Song, Z.Z.; Hu, X.Q. Development of sustained-release oxalic acid dihydrate microcapsules with different shell materials via a novel phase separation method: Performance evaluation and sustainable applications. *Colloids Surf. A Physicochem. Eng. Asp.* **2026**, *734*, 139420. [CrossRef]
14. Yang, G.C.; Zhang, Q.H.; Li, Y.; Ouyang, Y.S. Hydrophobic microcapsules modification of nitrogen-phosphorus flame retardant and its application in lignocellulosic materials. *J. Therm. Anal. Calorim.* **2022**, *147*, 13217–13229. [CrossRef]
15. Li, S.; Jiang, L.; Zhang, X.; Lin, Y. Preparation and characterization of phase change microcapsules emulsion for thermal energy storage and transportation. *Int. J. Heat Mass Tran.* **2022**, *191*, 122862. [CrossRef]
16. Ouarga, A.; Noukrati, H.; Iraola-Arregui, I.; Elaissari, A.; Barroug, A.; Ben Youcef, H. Development of anti-corrosion coating based on phosphorylated ethyl cellulose microcapsules. *Prog. Org. Coat.* **2020**, *148*, 105885. [CrossRef]
17. Sun, D.W.; Li, M.S.; He, H.Y.; Meng, S.Y.; Li, W.J.; Wang, J.X.; Liu, M.F.; Liu, S.Y.; Wang, Y.L.; Cui, S.P.; et al. Trigger mechanism investigations of microcapsules containing SAC for rapid self-healing mortars. *Constr. Build. Mater.* **2026**, *514*, 145591. [CrossRef]
18. Dong, Y.; Deng, J.Z.; Yan, X.X. Preparation of Tung Oil Microcapsules Coated with Chitosan Sodium Tripolyphosphate and Their Effects on Coating Film Performance. *Coatings* **2025**, *15*, 867.
19. Du, Z.X.; Li, C.L.; Wang, P.G.; Jin, Z.Q.; Tian, L.; Wang, A.S.; Zhang, M. Dual-trigger microcapsules for autonomous crack healing in marine concrete: Synergistic response to mechanical stress and chloride ions. *J. Build. Eng.* **2025**, *113*, 114151. [CrossRef]
20. Deng, J.Z.; Yan, X.X. Preparation of Tung Oil Microcapsules Coated with Chitosan-Arabic Gum and Its Effect on the Properties of UV Coating. *Polymers* **2025**, *17*, 1985. [CrossRef]
21. Radhakrishnan, A.; Panicker, U.G. Sustainable chitosan-based biomaterials for the future: A review. *Polym. Bull.* **2025**, *82*, 661–709. [CrossRef]
22. Bak, J. A comparative study on the rheological properties of concentrated xanthan gum in combination with gum arabic or gum arabic-based emulsion. *Int. J. Biol. Macromol.* **2024**, *265*, 131159. [CrossRef]
23. Chen, C.; Deng, S.Y.; Tian, H.X.; Kou, X.R.; Yu, H.Y.; Huang, J.; Lou, X.M.; Yuan, H.B. Novel bioactive sponge mats composed of oxidized bacterial cellulose and chitosan-gum Arabic microcapsules loaded with cinnamon essential oil for enhancing meat preservation. *Food Hydrocoll.* **2024**, *148*, 109496. [CrossRef]
24. Wang, Y.; Jie, G.L.; Xue, F. Preparation and study of n-docosane@tricyclodecane dimethanol diacrylate phase change microcapsules for potential application in thermal management composites. *J. Energy Storage* **2026**, *154*, 121291. [CrossRef]
25. Palmieri, G.F.; Bonacucina, G.; Di Martino, P.; Martelli, S. Spray-drying as a method for microparticulate con-trolled release systems preparation: Advantages and limits. I. Water-soluble drugs. *Drug. Dev. Ind. Pharm.* **2001**, *27*, 195–204. [CrossRef]
26. Hussain, S.M.; Ali, S.; Yilmaz, E.; Zahoor, A.F.; Javid, A.; Alshehri, M.A.; Shahzad, M.M.; Naeem, A.; Mahrukh. Microencapsulation: An Innovative Technology in Modern Science. *Polym. Adv. Technol.* **2025**, *36*, e70066. [CrossRef]
27. Dong, Y.; Deng, J.Z.; Yan, X.X. Effect of Chitosan Gum Arabic-Coated Tung Oil Microcapsules on the Performance of UV Coating on Cherry Wood Surface. *Coatings* **2025**, *15*, 873. [CrossRef]
28. Ma, L.; Xu, S.Y. Investigation on the restoration properties of wood oil microcapsules in wood coatings. *Prog. Org. Coat.* **2024**, *197*, 108853. [CrossRef]
29. Chang, Y.J.; Yan, X.X.; Wu, Z.H. Application and prospect of self-healing microcapsules in surface coating of wood. *Colloids Interface Sci. Commun.* **2023**, *56*, 100736. [CrossRef]
30. *GB/T 11186-2025*; Methods for Measuring the Colour of Coatings. Standardization Administration of the People's Republic of China: Beijing, China, 2025.
31. *GB/T 4893.6-2013*; Test of Surface Coatings of Furniture—Part 6: Determination of Gloss Value. Standardization Administration of the People's Republic of China: Beijing, China, 2013.
32. *GB/T 6739-2022*; Paints and Varnishes—Determination of Film Hardness by Pencil Test. Standardization Administration of the People's Republic of China: Beijing, China, 2022.
33. *GB/T4893.9-2013*; Test of Surface Coatings of Furniture—Part 9: Determination of Resistance to Impact. Standardization Administration of the People's Republic of China: Beijing, China, 2013.
34. *GB/T 4893.4-2023*; Test of Surface Coating of Furniture—Part 4: Determination of Adhesion by Cross-Cut. Standardization Administration of the People's Republic of China: Beijing, China, 2023.

35. *GB/T 1031-2009*; Geometrical Product Specifications (GPS)—Surface Texture: Profile Method Surface Roughness Parameters and Their Values. Standardization Administration of the People's Republic of China: Beijing, China, 2009.
36. Rule, J.D.; Sottos, N.R.; White, S.R. Effect of Microcapsules Size on the Performance of Self-Healing Polymers. *Polymer* **2007**, *48*, 3520–3529. [CrossRef]
37. Tomic, N.Z.; Mustapha, A.N.; AlMheiri, M.; AlShehhi, N.; Antunes, A. Advanced application of drying oils in smart self-healing coatings for corrosion protection: Feasibility for industrial application. *Prog. Org. Coat.* **2022**, *172*, 107070. [CrossRef]

**Disclaimer/Publisher's Note:** The statements, opinions and data contained in all publications are solely those of the individual author(s) and contributor(s) and not of MDPI and/or the editor(s). MDPI and/or the editor(s) disclaim responsibility for any injury to people or property resulting from any ideas, methods, instructions or products referred to in the content.